

Article pubs.acs.org/joc

Methyl Cation Affinities of Canonical Organic Functional Groups

Dora Kadish, Aaron D. Mood, Mohammadamin Tavakoli, Eugene S. Gutman, Pierre Baldi, and David L. Van Vranken*



Cite This: J. Org. Chem. 2021, 86, 3721-3729



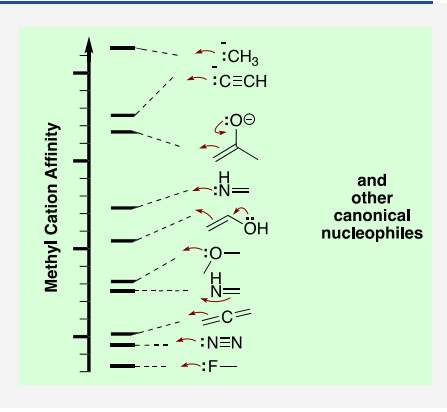
ACCESS

Metrics & More

Article Recommendations

Supporting Information

ABSTRACT: Methyl cation affinities are calculated for the canonical nucleophilic functional groups in organic chemistry. These methyl cation affinities, calculated with a solvation model (MCA*), give an emprical correlation with the Ns_N term from the Mayr equation under aprotic conditions when they are scaled to the Mayr reference cation (4- $MeOC_6H_4$ ₂ CH^+ (Mayr E=0). Highly reactive anionic nucleophiles were found to give a separate correlation, while some ylides and phosphorus compounds were determined to give a poor correlation. MCA*s are estimated for a broad range of simple molecules representing the canonical functional groups in organic chemistry. On the basis of a linear correlation, we estimate the range of nucleophilicities of organic functional groups, ranging from a C-C bond to a hypothetical tert-butyl carbanion, toward the reference electrophile to be about 50 orders of magnitude.



INTRODUCTION

Arrow-pushing is a fundamental tool for the description of polar organic reaction mechanisms. It begins with the deceptively simple act of choosing a nucleophilic pair of electrons and starting a curved arrow with those electrons.² After over almost a century of study, organic chemists still lack the ability to quantify and rank the nucleophilicity of all the canonical organic functional groups, ranging from C-C bonds to naked alkyl anions, against any reference electrophile in any reference environment (gas phase or solvent system). A complete and quantitative ranking of functional group nucleophilicities would empower the newest machine-learning algorithms, 4-6 new students of organic chemistry, and experienced practitioners in organic synthesis.

The Mayr Scale and Mayr Equation. Mayr and coworkers developed independent scales of nucleophilicity and electrophilicity for a wide range of polar compounds and a powerful equation for prediction of reaction rate constants: log $k_{20^{\circ}} = s_N s_E(E + N)$, where E and N are log-scale electrophilicity and log-scale nucleophilicity parameters, respectively, which can be plotted on a useful scale of reactivity order. 8,9 Mayr and his team determined Mayr E parameters for over 300 electrophiles, and within that range s_E is sufficiently close to unity that it could be neglected for sp²-centered electrophiles. Mayr N parameters and nucleophile-specific parameters s_N are available for over 1100 nucleophile/solvent combinations, 10 with far more diversity in comparison to the electrophilic functional groups. They have also been determined for π_{CC} nucleophiles on the basis of transition states for attack on a series of benzhydryl cations in CH₂Cl₂, 11 but transition states can be difficult to locate for highly exergonic or highly endergonic nucleophile-electrophile combinations. Experimental N and s_N parameters are plentiful, but for chemists looking for the nucleophilicity of a highly reactive free alkyl anion or a highly unreactive carbon-carbon bond, the necessary Mayr N and s_N parameters seem far out of reach.

 pK_{aH} is a Poor Predictor of Rates of Nucleophilic **Attack.** Most organic chemists refer to equilibrium pK_{aH} values—readily available from titrations—when they make quantitative comparisons between the reactivities of nucleophiles. 12 However, the correlation is not good. The accuracy can be improved by incorporating additional parameters such as oxidation potential and molar refractivity, but these data are often less common than pK_{aH} values. 13,14 The linear correlation between aqueous pK_{aH} and kinetic nucleophilicity parameters is good within each functional group class 15,16 but is poor across different classes of functional groups. ^{17,18,15} The correlation between pK_{aH} and the predicted log k^{19} for nucleophilic addition is also poor in organic solvents (Figure 1). 20 R^2 is 0.09 for H₂O and 0.35 for DMSO. 21 A second limitation to estimating nucleophilicity from pK_{aH} is that experimental pK_{aH}values cannot be directly measured for functional groups far less acidic than the solvent or far more acidic than the conjugate acid of the solvent. 22,23 Mayr and coworkers have determined nucleophilicity parameters over a much wider range in comparison to the available experimental

Received: September 30, 2020 Published: February 17, 2021





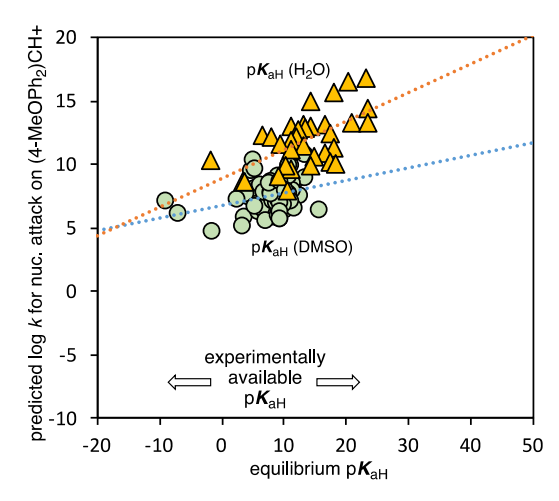


Figure 1. pK_{aH} correlates poorly with rates of nucleophilic attack. Nucleophilicity (log k from the Mayr equation) toward (4-MeOC₆H₄)₂CH⁺ correlates with equilibrium basicity ($R^2 = 0.34$ for both H₂O and DMSO). For a list of the nucleophiles, see Table S1 in the Supporting Information.

 pK_{aH} values for organic functional groups. pK_{aH} values in DMSO can be accurately predicted with electronic structure calculations, ^{24–27} but it is not clear whether it is better to estimate nucleophilicity using accurately calculated pK_{aH} values that correlate poorly with nucleophilicity, or to estimate nucleophilicity on the basis of a different value that is readily accessible.

Does MCA* Correlate Better than pK_{aH} with Rates of Nucleophilic Attack? Hydride anion affinity has previously been correlated with the electrophilicity of quinones, ²⁸ and recently we reported a linear correlation between methyl anion affinity (MAA*), calculated with a continuum solvation model, and the Mayr electrophilicity parameter. ²⁹ The success of this correlation invites a similar exploration of the relationship between methyl cation affinities and nucleophilicity. Hine has previously suggested that "rate-equilibrium correlations tend to improve as the differences in structure between the compounds whose reactions are being compared are decreased." Motivated by Hine's statement, we set out to explore methyl cation affinity (MCA) as an alternative to pK_{aH} by converting readily calculated methyl cation affinities to a Mayr scale.

Does Methyl Cation Affinity Correlate with Nucleophilic Addition Rates? Methyl cation affinities (MCAs) are related to methyl transfer affinities introduced by Hine and Weimar in 1965.30 Calculated MCAs31,32 have been tabulated for organocatalysts within narrow ranges of nucleophilic functional groups: substituted phosphines,³³ amines and 4aminopyridines,³⁴ and sterically hindered pyridines.³⁵ MCAs have been shown to give a ood correlation with nucleophilicity. In 1983, Pellerite and Brauman correlated the methyl cation affinities of eight anionic nucleophiles (Br-, Cl-, AcO-, CD₃S⁻, t-BuO⁻, MeO⁻, HCC⁻) with the intrinsic barriers for S_N2 displacement of methyl halides in the gas phase.³⁶ Mayr and co-workers have shown that ground-state thermodynamics is insufficient for an accurate prediction of regiochemistry in the case of ambident nucleophiles.³⁷ In those cases intrinsic barriers offer critical insight into

When MCA is defined as the negative of the free energy change for reaction of H₃C⁺ with nucleophiles (Figure 2A), a

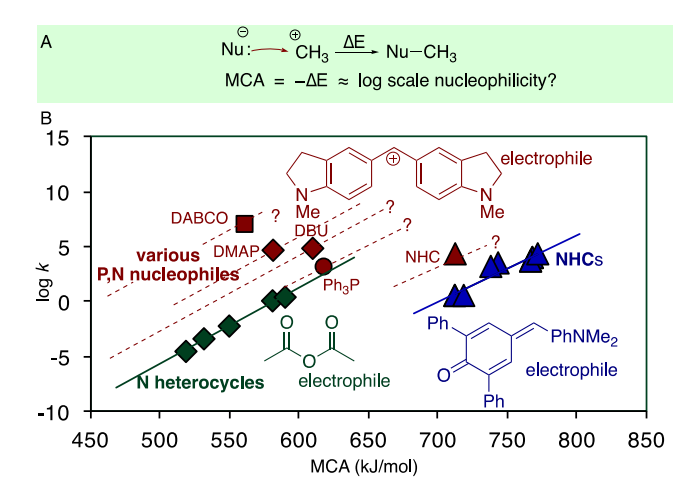


Figure 2. Calculated gas-phase MCA appears to correlate linearly with log k within nucleophilic functional group classes (\blacksquare , \spadesuit , \spadesuit) but not across different functional group classes (red symbols).

higher affinity correlates intuitively with lower activation energy and higher rates of nucleophilic attack. MCAs have been shown to correlate with $\log k$ for various reactions (Figure 2B).³⁸ In 2008, Zipse and co-workers showed that calculated MCAs for pyridine derivatives correlate with the $\log k$ values for Steglich acylations, where addition of the amine to the carbonyl is rate-determining (Figure 2B, green points).³⁹ For *p*-quinone methide electrophiles it was shown that MCAs correlate with the $\log k$ values for addition of N-heterocyclic carbenes to quinone methides (Figure 2B, blue points) and other similar electrophiles.^{40,41} The functionally diverse classes of nucleophiles DABCO, 4-DMAP, DBU, and Ph₃P would be expected to fall on different lines (Figure 2B, red points).^{42,43}

How Does One Choose a Reference Scale for Nucleophilicity? Mayr has previously noted the existence of a nucleophilicity scale versus an electrophile with E=0 (for the 4,4'-dimethyoxybenzhydryl cation), where the Mayr equation yields $\log k_{20} = N s_{\rm N}$. The 4,4'-dimethyoxybenzhydryl cation is rated by Mayr as a five-star reference cation which is expected to give an accurate prediction of $\log k$. In spite of the limitations of a single reference electrophile, we set out to explore the correlation between calculated methyl cation affinities—unbounded by solvent reactivity, solubility, or other experimental parameters—and $\log k$ for attack on the 4,4'-dimethyoxybenzhydryl cation, calculated from the Mayr parameters and the Mayr equation.

Why Choose Methyl Cation Affinity to Match a Scale Determined by a Stabilized Benzhydryl Cation? An important goal of this work is to translate trends in methyl cation affinity to trends in nucleophilic addition rates toward a hypothetical cation with Mayr E = 0, while minimizing the confounding effects of sterics. Brauman and co-workers have previously shown that proton affinity correlates with methyl cation affinity, 45 but methyl cations seem to be more apt models for organic reactivity. The main advantange of methyl cation affinity over 4,4'-dimethyoxybenzhydryl cation affinity is computational economy, attributable to fewer atoms. Geometry optimizations are further simplified because the methyl group has three fewer degrees of freedom in comparison to a benzhydryl group. Steric effects can easily dominate over the inherent nucleophilicity of many functional groups, 46 but the diminutive methyl cation minimizes steric effects. In this work we show that methyl cation affinity is a predictor of nucleophilicity toward the Mayr reference cation 4,4'-dimethyoxybenzhydryl cation (E=0).

■ RESULTS AND DISCUSSION

Solvation Models Are Essential for Correlation of MCA with Mayr Ns_N. In our previous work²⁹ on electrophilicity we showed that PBE0(disp)/def2-TZVP $COSMO(\infty)$ gave the same or slightly better correlation between calculated methyl anion affinity (MAA) and Mayr E in comparison to B3LYP/6-311++G(3df,2pd) SMD(DMSO) used in Mayr's prior work. Both levels of theory gave MCA* with similar correlations to Mayr E. In that work on electrophiles, MAA* calculated with COSMO(∞) were similar to MAA* calculated with COSMO(DMSO). We chose to use the $COSMO(\infty)$ model for the calculation of methyl anion affinities with the expectation that it might maximize any beneficial effect of the solvation model. In this work on nucleophiles, we started with a test set of 10 different nucleophiles spanning about 25 orders of magnitude, almost the full range of available Mayr Ns_N (Figure 3A). The starting

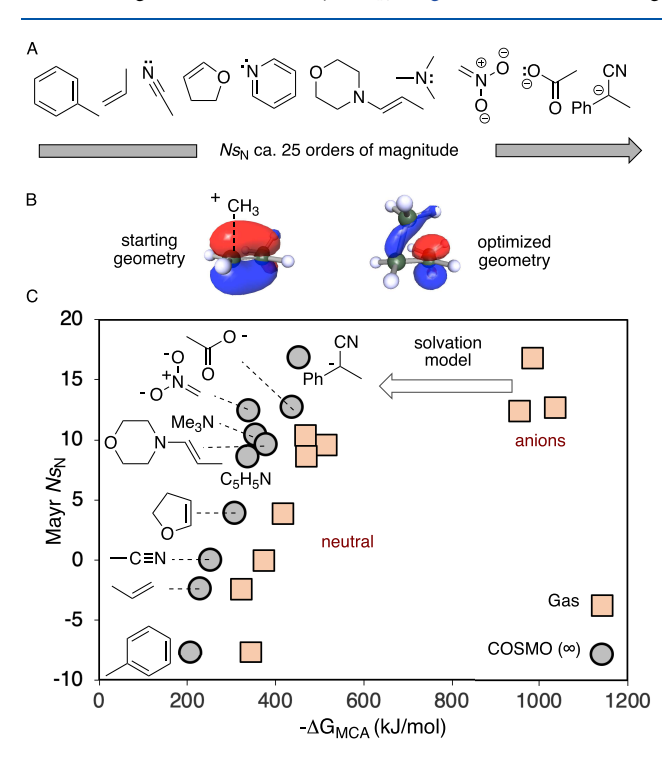


Figure 3. Correlation of MCA* with Ns_N for a test set of nucleophiles. (A) The test set of anionic and neutral nucleophiles covered a broad range of Mayr Ns_N . (B) Starting geometries for the products were chosen so that the newly formed H_3C-C was aligned with the nucleophile HOMO (e.g., H_3C^+ -propene adduct). (C) A solvation model leads to better correlation of MCA with Mayr Ns_N .

geometries for optimization of the products of methyl cation addition were initially arranged so that the newly formed bond to the CH₃ group was aligned with the nucleophile HOMO of the nucleophile reactant: for example, a lone pair or a π system (centered on the atom with the highest coefficient) (Figure 3B).

As in a previous study on MAAs, MCAs give much better correlations with Ns_N when a single-point solvation energy such as SMD or COSMO is added to the free energy (Figure 3C). The correlation was slightly tighter when geometries were

optimized with the $COSMO(\infty)$ solvation model and thermochemistry from frequency calculations was excluded (Figure S2 in the Supporting Information). We define MCA* as the methyl cation affinity $(-\Delta E_{MCA})$ calculated with a solvation model in order to distinguish it from the traditional notion of a gas-phase methyl cation affinity (MCA).

It seemed plausible that better correlation would be obtained if the products were constrained throughout the optimization to geometries resembling transition states. To explore this idea, products from acyclic conjugated π nucleophiles (nitrile anion, nitromethane anion, enamine) were optimized with the newly formed H_3C-C bond constrained to the orientation of the starting material HOMO, with a 90° torsion angle versus the atoms in the nucleophile HOMO. Without a constraint, the lowest energy conformation of the CH_3^+ -nitromethide adduct places the methyl group in plane with the nitro group and orthogonal to the critical π system (Figure 4). The difference in MCA* was

constrained NOT

$$H^{+}C \subset H$$
 $H^{+}C \subset H$
 $H^{+}C \subset H$

Figure 4. When products of acyclic conjugated π systems were constrained during optimization with the newly formed H_3C-C bond aligned with the nucleophile HOMO, it made little difference, relative to the large magnitude of MCA*.

≤7 kJ/mol (Supporting Information). With more data, it became apparent that the constraints were not providing an advantage; therefore, constraints were not applied when MCA* was calculated for the Mayr nucleophiles.

It is not expected that rate constants should be calculable with thermodynamic terms such as MCA* while intrinsic barriers are ignored. Hoz and co-workers have calculated activation energies for the identity reactions (ΔG^{\ddagger} , in eq 1) at the G2 level of theory and found a decrease in the barrier as X moves to the right in the Periodic Table: X = MeCH $_2^-$ (44.7 kcal/mol) < MeNH $^-$ (29.3 kcal/mol) < MeO $^-$ (19.5 kcal/mol) < F $^-$ (11.6 kcal/mol). A better correlation with Mayr $Ns_{\rm N}$ might, therefore, be achievable by combining calculated methyl cation affilities with intrinsic barriers, but that is beyond the scope of this work.

$$^{-}X:+H_{3}C-X \xrightarrow{\Delta G^{\ddagger}} X-CH_{3} + :X^{-}$$
 (1)

Correlations Between MCA* and Nucleophilicity (Mayr Ns_N). Having shown that MCA*s correlate well with the Ns_N term in the Mayr equation for the test set of 10 nucleophiles, we set out to extend that analysis to a much fuller set of structurally diverse nucleophiles. To date, Mayr and Ofial have reported Mayr N and s_N parameters for over 1200 different nucleophile/solvent combinations—a much broader range of functional groups in comparison to the corresponding electrophiles. The nucleophilic functional groups include molecules from over 61 general classes of nucleophilic functional groups. These functional groups include (i) nonbonding lone pairs (alkoxide anions, alcohols, carboxylates, carbonates, oxyhalides, peroxy anions, phenolates, aliphatic amines, aromatic amines, imines, amidines, guanidines, azoles, hydrazines, hydroxylamines, isoamides, isothioamide, isothioureas, nucleobase anions, pyridines, thiocyanate, nitrites,

cyanate, azides, sulfite anions, phenylsulfinate anions, thioacetate anions, xanthate anions, dithiocarbamate anions, phosphines, phosphites, and halide anions), (ii) π systems (alkenes, arylboronates, alkynes, allylsilanes, allylboronates, allylmetal species, arenes, sulfonylcarbanions, stabilized enolates, nitronates, N-heterocyclic carbenes, enol ethers, enamines, enamides, ynamides, diazo compounds, isonitriles, metal π complexes, metallocenes, vinylsilanes, ylides, amide anions, and imide anions), and (iii) σ bonds (hydridoborates, alkylsilanes and arylsilanes, hydridometal donors, H–C donors, diazaphospholes (H–P donors), and alkylboronates). The rich Mayr data set often contains many nucleophiles within a given class; for this investigation, an attempt was made to choose just one type of nucleophile from each class.

The MCA* calculations were meant to quantify the typical depictions of nucleophiles without explicit solvent interactions and without the effects of sterics. Where possible, we tried to avoid parameters associated with sterically demanding nucleophiles, such as N-heterocyclic carbenes. For this work, we tried to avoid σ bond nucleophiles. σ Bond nucleophiles are associated with high intrinsic barriers, which are not considered. σ Bond nucleophiles also introduce issues of translational entropy arising from transformations that generate two products instead of one. We calculated MCA* values of 98 molecules from the Mayr-Ofial database encompassing the entire range of nucleophilicities, from the least reactive nucleophile toluene ($Ns_N = -7.7$) to the most reactive nucleophile Ph(NC)MeCK ($Ns_N = 16.8$) (Table S6 in the Supporting Information). An attempt was made to capture as many of the elementary organic functional groups as possible, but seeing a weak correlation for nucleophiles with heavier atoms, such as phosphines and thiocyanate anions, we did not further pursue phosphonium ylides or organometallic complexes.

It is common for organic chemists to depict nucleophiles without solvation shells and/or nucleophiles unbonded to counterions. As long as those misrepresentations are common, it is important to quantify their reactivity. Mayr and his team are careful to report nucleophilicity parameters for nucleophile/solvent combinations because they are not independent. Mayr depicts negatively charged species as free anions, but his group carefully minimizes and accounts for the effects of alkali counterions using, for example, noncoordinating counterions, crown ethers, phosphazene bases, and coordinating solvents such as DMSO. We calculated MCA* only for Mayr's nucleophile/solvent combinations determined in aprotic solvents in order to minimize the effects of solvent reorganization that would require the inclusion of explicit solvent molecules in the MCA calculations.

MCA*s calculated for these nucleophiles were found to correlate well with the Mayr nucleophilicity term Ns_N (Figure 5) in most cases. For most resonance-stabilized ambident nucleophiles composed of second-row atoms (enolates, enamines, nitronate anions, amide anions, enamines, and enol (ethers)), the MCA* for the known site of attack by carbon electrophiles correlated well with the Mayr Ns_N . Most of the nucleophiles fell on one line (gray points). Empirically, some of the anionic nucleophiles where observed to fall on a different line (green points), specifically those in which the charge was localized on the nucleophilic atom. Many of those S and O nucleophiles were noted by Hoz to proceed with lower intrinsic barriers, with the result that they react more quickly than expected from the thermodynamic driving force.

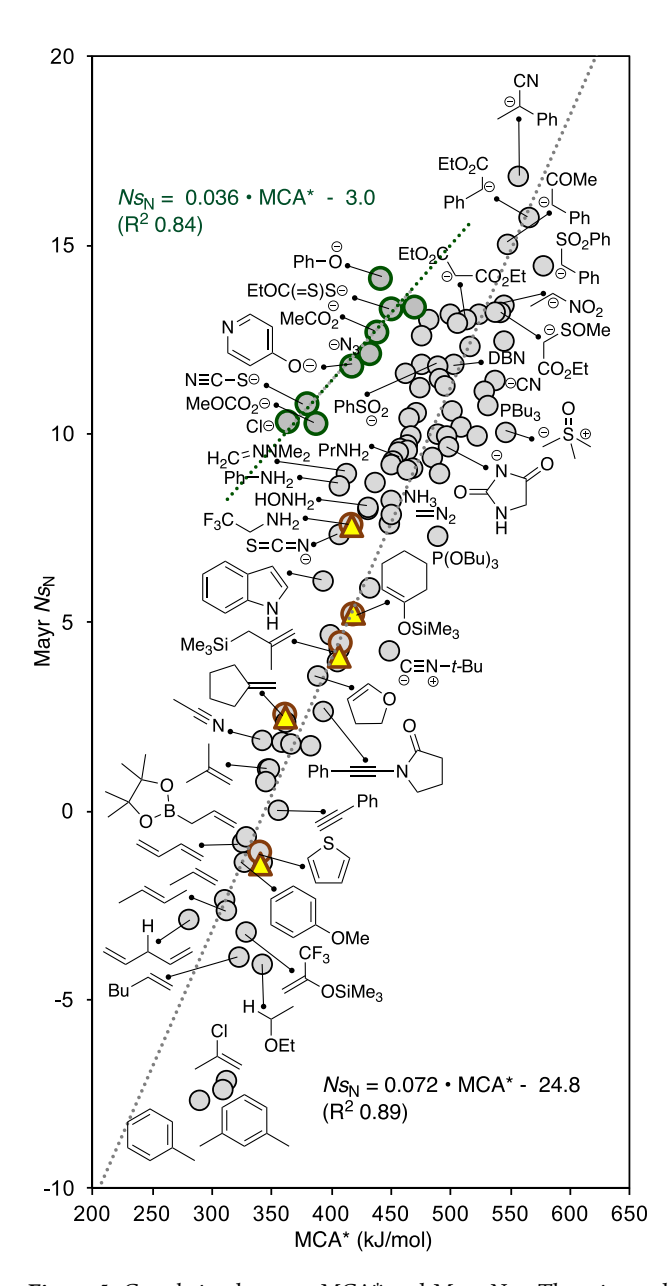


Figure 5. Correlation between MCA* and Mayr Ns_N . There is good correlation between the calculated MCA* (PBE0/def2-TZVP COSMO(∞) opt) and Mayr Ns_N across his full range of organic nucleophiles. Legend: circles, Mayr Ns_N (gray, organic solvents; blue, water); triangles, experimental log k versus (4-MeOC₆H₄)₂CH⁺.

Surprisingly, the anionic atom line was not quite parallel, possibly due to the relatively small range and small number of points. Mayr $Ns_{\rm N}$ values are not available in aprotic solvents for substantially more reactive or substantially less reactive heteroatomic anions. Naked carbanions and naked enolates and alkyllithiums are common mis-representations of the true nucleophiles present under experimental conditions; the MCA*s plotted in Figure 5 quantify those common misrepresentations and provide a basis for discussion.

Is it valid to correlate MCA* with calculated log k (from the Mayr equation) instead of experimental log k? Few experimental log k values are available for the reactions of nucleophiles versus $(4\text{-MeOC}_6\text{H}_4)_2\text{CH}^+$ (red-yellow triangles),

but as expected, experimental log k values were within 0.3 log unit of the value calculated from Mayr Ns_N (red-gray circles).

The most dramatic outliers, over 3 orders of magnitude $(Ns_{\rm N})$ off the main fitted line, include N,N-dimethylhydrazone of formaldehyde (+3.6, N-alkylation), ethyl phenylacetate enolate (+3.6), aniline (+3.2), malononitrile anion (+3.1), 2-chloropropene (-5.4), ethyl ether $\alpha\text{-C-H}$ (-4.7), toluene (-4.4), $Me_2S(O)CH_2$ (-4.4), t-BuNC (-3.5), and $(n\text{-BuO})_3P$ (-3.2). The correlation deviates from linearity at the bottom end of the scale, and it is not clear if the deviation is systematic for the weakest nucleophiles, because $Ns_{\rm N}$ parameters below -5 are available for only three nonhydridic nucleophiles: toluene, m-xylene, and 2-chloropropene. A linear correlation overestimates $Ns_{\rm N}$ for the weakest nucleophiles parametrized by Mayr.

The linear correlation of MCA* to Mayr Ns_N is poor for nucleophiles with MCA* values below ca. 325 kJ/mol. If the overestimation of reactivity is systematic for weak nucleophiles, then the MCA* should reflect an upper limit to the nucleophilicity for those cases.

Quantifying the Reactivity of the Canonical Nucleophiles on the Mayr Scale. Having shown that MCA* (PBE0/def2-TZVP COSMO(∞)) correlates with Mayr Ns_N , we set out to use those correlations to estimate the full range of log-scale nucleophilicities of the common canonical functional groups in organic chemistry (Figure 6). On the scale of an electrophile where Mayr E=0, the range of nucleophilicity from a *tert*-butyl anion to an ethane C–C bond is about 50 orders of magnitude. For ambident nucleophiles we were careful to include cases where the regiochemistry was known and the correlation between MCA* and Mayr Ns_N was good: for example, C-alkylation of enolates, nitronates, nitrile-stabilized carbanions, enol (ethers), and enamines.

The Less Reactive Parts of a Canonical Functional Group. Among the most interesting nucleophilic functional groups in Figure 6 are those that do not represent the most reactive "part" of the Lewis depiction. For example, Mayr Nand s_N parameters are available for the α -C-H bonds of diethyl ether, but not the oxygen atom (Figure 7A). Similarly, Mayr Ns_N parameters are available for imines, but it is not clear which part of the imine is more reactive—the lone pair or the π bond—nor by how much (Figure 7B). The imine and related functional groups are not considered ambident nucleophiles because addition to the nitrogen lone pair would give the same N-C bond as addition to the C=N π bond. For small molecules, the frontier orbitals are generally recognizable as one of three components of Lewis structures: electron lone pairs, π bonds, and σ bonds. It is the generally held wisdom that when all else is equal the relative order of reactivity should be lone pair > π bond > σ bond. To facilitate comparison of these different arrow-pushing representations, we calculated MCA* values for geometries that best corresponded to the interaction of a methyl cation with the appropriate frontier orbital, e.g. either the imine lone pair or the imine π bond, in Figure 7B. In some cases, detailed in the following sections, the geometries required careful consid-

Imine π **Bond versus Imine Lone Pair.** A stationary point was found corresponding to addition of H_3C^+ to the C=N π bond of formaldimine (Figure 8). A closely related but more stable hydride-bridged structure was found corresponding to hydride transfer from the H_3C group to the imine carbon. Some of that C-H donation in the hydride

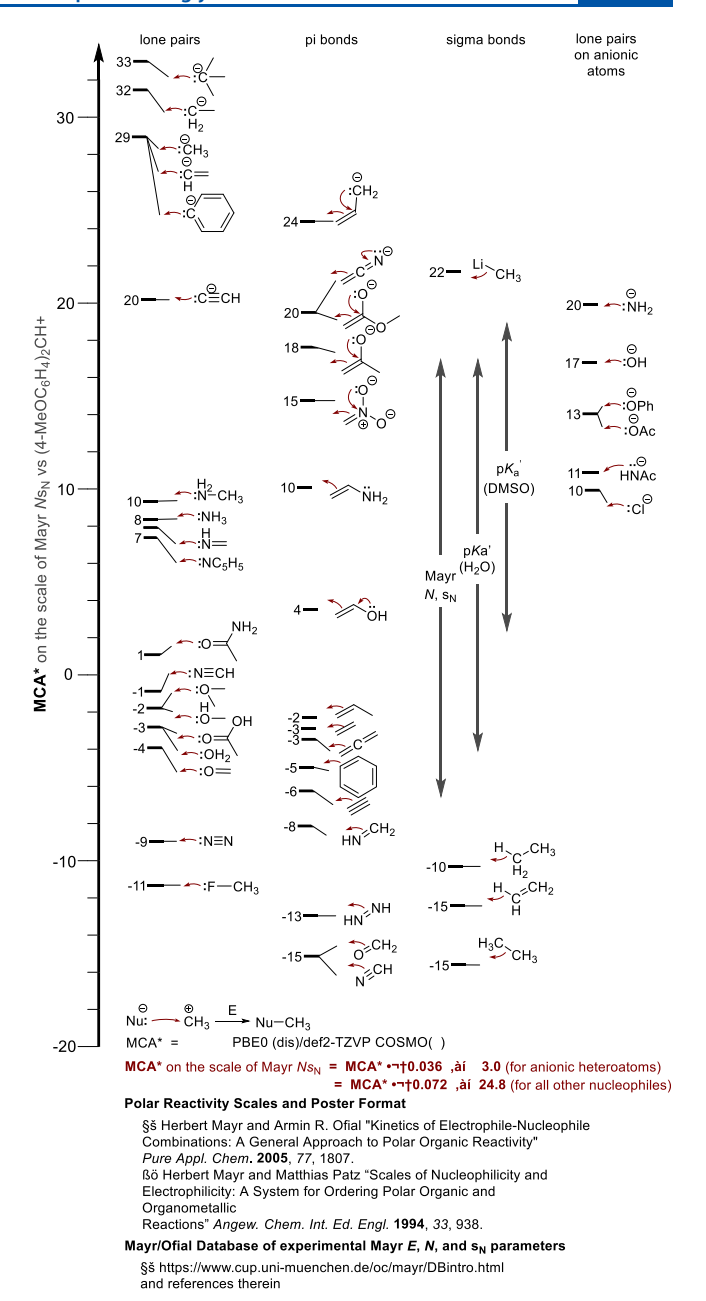


Figure 6. Methyl cation affinities (MCA*s) of canonical functional groups plotted on the scale of Mayr Ns_N in aprotic solvents toward (4-MeOC₆H₄)₂CH⁺. The range of experimentally measured parameters, often used to correlate with nucleophilicity, is shown for comparison.

Figure 7. Can MCA* be used to distinguish quantitatively between the reactivity of different "parts" of a molecule?.

bridge structure could be present in the π adduct structure; therefore, an MCA* of 211 kJ/mol for the C=N π bond represents an upper limit. Thus, the MCA* value for an imine π bond is 18 orders of magnitude lower than the MCA* value for an imine lone pair on the scale of Mayr $Ns_{\rm N}$.

Hydrogen Cyanide π Bond versus Hydrogen Cyanide Lone Pair. The reaction of an electrophile with a cyano group can be represented with a curved arrow that starts with either

Figure 8. MCA*s for the imine π bond are lower than those of the imine lone pair. The MCA* for a canonical C=N π bond was based on the unbridged π adduct.

the CN π bond or the nitrogen lone pair (Figure 9A). For hydrocyanic acid, two degenerate HOMOs correspond to

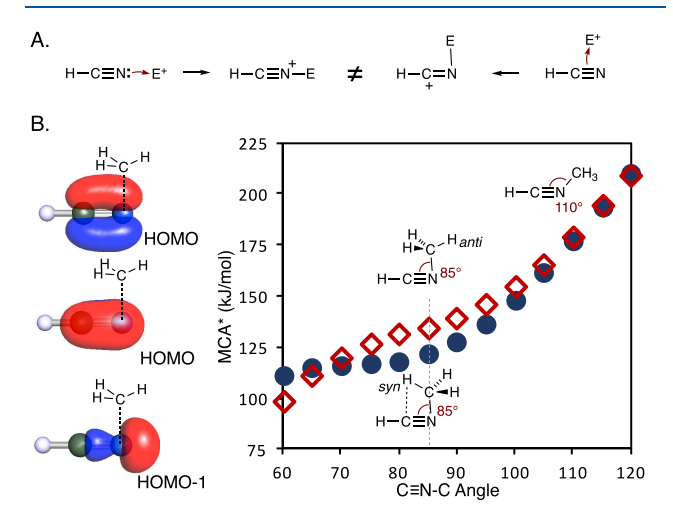


Figure 9. (A) Different depictions of attack of HCN on a methyl cation correspond to interactions with frontier orbitals of different symmetry. (B) Variation in MCA* with H_3C-N-C angle. A reference angle for the MCA* for addition of CH_3^+ to $C \equiv N \pi$ was set at 85°. The *anti* conformation was chosen to avoid the stabilizing interaction methyl C-H.

orthogonal π bonds, whereas the HOMO-1 corresponds to the lone pair (Figure 9B). Without constraints, the adduct of CH_3^+ and $HC \equiv CH$ minimizes to a three-membered ring consistent with approach of the methyl cation from the middle of the triple bond. The nitrogen lone pair of HCN complicates the situation for the addition of an electrophile to a cyano group. The adduct of $HC \equiv N$ and CH_3^+ minimizes to a linear conformation, resembling addition the nitrogen lone pair (HOMO-2). While Figure 9A shows the optimal geometry for interaction with the nitrogen lone pair, Figure 9B highlights how varying the trajectory in order to maximize interactions with a π -like HOMO affects the energy.

In order to maximize interactions with a π-like HOMO and minimize interactions with the nonbonding HOMO-1, MCA*s were explored for HC≡N−CH₃ angles between 60 and 120°. There was no local minimum as with HC≡CH. The CH₃ group prefers a *syn* conformation in which one of the H−C bonds can interact with the nitrile carbon (Figure 9B, red diamonds), but this type of interaction might not be general for all electrophiles; therefore, one of the C−H bonds of the methyl group was constrained to be *anti* to the C≡N bond. For this *anti* conformation, HC≡N−CH₃ angles between 65 and 85° led to similar MCA*s, within 3 kJ/mol; therefore, 85°

was chosen as the reference angle for the MCA* for a nitrile π bond.

C–H Bonds versus π **C–C Bonds.** No constraints were used in the determination of MCA* for the C–H bond of ethane (176.0 kJ/mol or –11 on the scale of Mayr Ns_N); the product minimizes to a geometry consistent with $H_3C-H\cdots^+CH_2CH_3$. To determine the MCA* for an ethene C–H bond, it is necessary and sufficient to constrain the $H_3C-H-C=C$ torsion angle to 180° to minimize interaction of the methyl cation with the π system. The resulting MCA* for $C(sp^2)-H$ is 125.7 kJ/mol, which is 4 orders of magnitude lower than that of the $C(sp^3)-H$ bond of ethane on the scale of Ns_N .

The C-H bond of ethyne is extremely non-nucleophilic. Full transfer of a hydride from ethyne to a methyl cation is uphill in energy by 305 kJ/mol (Figure 10A). At the



Figure 10. The reaction of the ethyne C–H bond with a methyl cation is endothermic.

PBE0(disp)/def2-TZVP level of theory, no net interaction was observed beyond $H_3C-H-CC$ angles of 145° (Figure 10B). At an angle of 145° , the MCA* was -24 kJ/mol, probably arising to some extent from interactions with the π system. $H_3C-H-CC$ bond angles minimize net interactions with π HOMOs, but at the PBE0(disp)/def2-TZVP level of theory, no net interaction was observed beyond. The MCA* for an ethyne C-H bond was -24 kJ/mol at a $H_3C-H-CCH$ angle of 145° , probably arising to some extent from interactions with the π system. The MCA* for an ethyne C-H bond is certainly lower than -24 kJ/mol (Mayr Ns_N -25) but not less than a lower bound of -305 kJ/mol (Mayr Ns_N -44) which does not take entropy into account.

Formaldehyde *π* **Bond versus Formaldehyde Lone Pair.** As with the reaction of an electrophile with a cyano group, the reaction of an electrophile with a carbonyl oxygen can be represented with a curved arrow that starts with either the carbonyl π bond or the carbonyl lone pair (Figure 11A). For formaldehyde, the HOMO corresponds to a nonbonding lone pair (HOMO and HOMO-2), whereas the HOMO-1 corresponds to the π bond. Without constraints, the adduct of CH_3^+ and $H_2C=CH_2$ minimizes to a three-membered ring consistent with approach of the methyl cation from the middle of the double bond. The oxygen lone pairs complicate the situation for $H_2C=O$. Without constraints, the adduct of CH_3^+ and formaldehyde minimizes to a planar conformation, resembling addition to the carbonyl lone pair (HOMO and HOMO-2) (Figure 11B).

In order to maximize interactions with the π -like HOMO-1 and minimize interactions with the nonbonding HOMO and HOMO-2, the structure was constrained to a conformation with C_s symmetry, with one of the C–H bonds of the methyl cation *anti* to the CH₂ (Figure 11B). Obtuse C=O–C angles led to significant interaction with the nonbonding HOMO-2. With acute C=O–C angles, the methyl H–C bond strongly

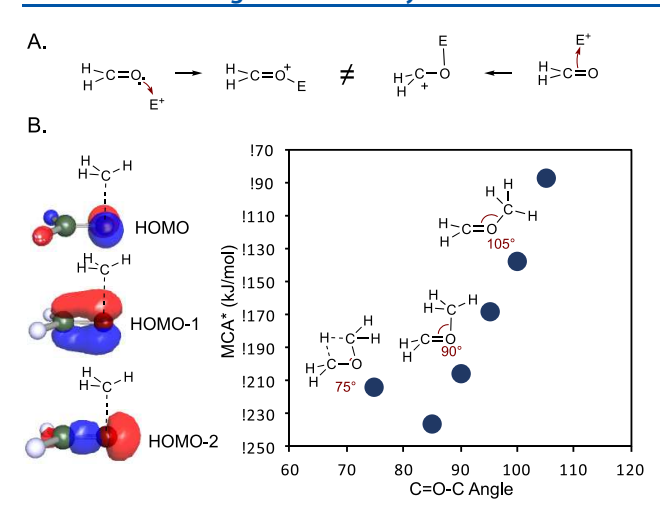


Figure 11. (A) Different depictions of attack of H_2CO on a methyl cation correspond to interactions with frontier orbitals of different symmetry. (B) Variation in MCA* with H_3C-O-C angle. The *anti* conformation was chosen to avoid the stabilizing interaction methyl C-H. A reference angle for the MCA* for addition CH_3^+ to C=O π was set at 90°.

prefers to be directed toward the carbonyl carbon, ultimately leading to $H_2C-O-CH_2$ with a hydrogen bridging between the carbon atoms. To avoid this interaction, we assigned the MCA* for a formaldehyde C=O π bond to correspond to approach from a 90° angle.

Ethane has two degenerate HOMOs that correspond to C–H bonds; the HOMO-1 orbital corresponds to the C–C σ bond (Figure 12A). The MCA* for the C–C bond of ethane was based on a stationary point for an linear geometry corresponding to end-on attack oriented 180° from the C–C bond (Figure 12B).

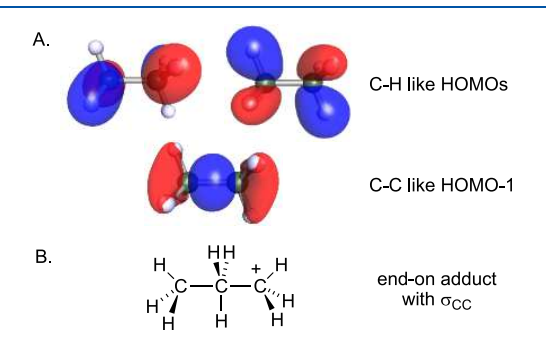


Figure 12. (A) MCA* for the ethane C–C bond was based on a linear trajectory. (B) The frontier orbitals of ethane.

To the extent that methyl cation affinity, calculated with solvation, correlates linearly with solution phase reactivity, we begin to see the range of nucleophilicity of the canonical organic functional groups referenced to a cation with Mayr E=0, a range covering 50 orders of magnitude—more than twice the log-scale range of experimental $Ns_{\rm N}$ or $pK_{\rm aH}$ values. It may seem gratuitous to calculate MCA* for naked alkyl anions. They have little relevance to Terran laboratory conditions, ^{49,50} but there is evidence for the ethynide anion and even the exquisitely sensitive CH_3^- anion in the atmosphere of Titan, here within our solar system.

It is important to remember that a choosier, less reactive reference electrophile such as cinnamonitrile would have led to a hypothetical range broader than 50 orders of magnitude (if unbounded by the limits of molecular diffusion). Likewise, a more aggressive reference electrophile such as an unsubstituted benzhydryl cation would have led to a narrower range of nucleophilicities. The relative and absolute nucleophilicities are expected to change from one electrophile to another, but the rank order of nucleophilicity is expected to be relatively constant, except on comparison of the anionic heteroatoms, which were fitted to a different linear function. MCA* strongly underestimates Ns_N for toluene, m-xylene, and 2-chloropropene; if this trend is general, then MCA* should should be an considered upper limit for values < 4 on the Mayr scale.

Caution in Interpreting MCA* Converted to the NsN **Scale.** The main goal of this work is to express nonintuitive values, rooted in thermodynamics, on a scale that correlates with intuitive log-scale reaction rates. The thermodynamic values could be pK_{aH}, MCA*, HOMO-LUMO interaction energies, or other readily available values. The Mayr Ns_N scale is the best available and is backed by decades of careful experimental work. MCA* is only loosely correlated with Ns_N and cannot be separated into the individual components of Nand s_N that are necessary to calculate solution -phase rate constants for the broad types of electrrophiles that interest most organic chemists. MCA* is scaled to a hypothetical cation with Mayr E = 0 (as a mathematical convenience), while E = 0 for the 4,4'-dimethyoxybenzhydryl cation, MCA* can offer no mechanistic insight into the reaction of a nucleophile with the 4,4'-dimethyoxybenzhydryl cation.

CONCLUSION

MCA* values were calculated for a wide range of simple molecules representing most of the canonical functional groups in organic chemistry, including C–H bonds, C–C bonds, C=N π bonds, etc. MCA* cannot fully embody any of the various changes in geometry, solvation, or charge distribution in the transition state, particularly for S_N2 transition states; therefore, readers should be careful not to misconstrue MCA* as a replacement for solution-phase kinetic parameters. There is a pressing need for more experimentally determined reactivity parameters. In the absence of kinetic data, converting MCA* to the Mayr Ns_N scale allows chemists to consider nucleophilicity in a familiar context and offers a glimpse of the impressive range of nucleophilicities for functional groups ranging from C–C σ bonds to the hypothetical tert-butyl carbanion.

EXPERIMENTAL SECTION

Computational Methods. Electronic structure calculations were carried out using Turbomole. Si Initial geometries for nucleophile reactants were optimized in the gas phase using the BP86 functional and the SV(P) basis set. Convergence energy criteria for SCF and geometry calculations were set at 10^{-6} hartree or lower. Final geometry optimizations were performed using the dispersion-corrected PBE0^{S5} functional (gridsize m3) with DFT-D3 Becke–Johnson damping set using the def2-TZVP basis set. Energies in hartree were converted to kJ/mol for the manuscript (1 hartree = 2625.5 kJ/mol). When indicated, solvation was included using the COSMO solvation model 75,58 with ε = infinity with the inner cavity removed. Geometry optimizations were then carried out to minimum energy stationary points without constraints. Visualization of the nucleophile HOMO was used to approximate a starting geometry for the methyl adduct as described below.

The starting geometries for optimization of the products of methyl cation addition were initially arranged so that the newly formed bond

to the CH₃ group was aligned with the nucleophile HOMO of the nucleophile reactant: for example, a lone pair or a π system (centered on the atom with the highest coefficient). The geometries were then optimized at the BP86/SV(P) level and finally at the PBE0(disp)/def2-TZVP level of theory without constraints, unless described specifically in the text.

For the canonical functional groups in Figure 6 that do not correspond to the most reactive part of the molecule, constraints were applied to the methyl adducts during geometry optimization, specifically CN π bonds (vs N lone pairs), C=O π bonds (vs O lone pairs), C-H bonds (vs C=C π bonds), C-C bonds (vs C-H bonds). All of those constraints are described in detail toward the end of the Results and Discussion.

ASSOCIATED CONTENT

Supporting Information

The Supporting Information is available free of charge at https://pubs.acs.org/doi/10.1021/acs.joc.0c02327.

Computational details and methods (PDF) Additional figures (XLSX)

AUTHOR INFORMATION

Corresponding Author

United States

David L. Van Vranken — Department of Chemistry, University of California, Irvine, California 92697, United States;
orcid.org/0000-0001-5964-7042; Email: david.vv@uci.edu

Authors

Dora Kadish — Department of Chemistry, University of California, Irvine, California 92697, United States Aaron D. Mood — Department of Chemistry, University of California, Irvine, California 92697, United States Mohammadamin Tavakoli — Department of Computer Science, University of California, Irvine, California 92697,

Eugene S. Gutman – Department of Chemistry, University of California, Irvine, California 92697, United States

Pierre Baldi – Department of Computer Science, University of California, Irvine, California 92697, United States

Complete contact information is available at: https://pubs.acs.org/10.1021/acs.joc.0c02327

Notes

The authors declare no competing financial interest.

ACKNOWLEDGMENTS

We are grateful to Professor Herbert Mayr for helpful comments and discussion. This work was made possible by the generous support of NSF CHE 1955811 and DARPA HR0011-15-2-0045. A.D.M. and M.T. were supported by NSF NRT-1633631. Calculations were carried with the assistance of Dr. Nathan Crawford using the Greenplanet cluster supported by NSF CHE-0840513.

REFERENCES

- (1) O'Hagan, D.; Lloyd, D. The Iconic Curly Arrow. Chemistry World 2010, 7, 54-57.
- (2) Saltzman, M. Arthur Lapworth. The genesis of reaction mechanism. J. Chem. Educ. 1972, 49, 750-52.
- (3) Harris, J. M.; McManus, S. P. 1. Introduction to Nucleophilic Reactivity. In *Nucleophilicity*; Harris, J. M., McManus, S. P., Eds.; ACS Publications: Washington, DC, 1987; pp 1–20.

- (4) (a) Kayala, M. A.; Azencott, C.-A.; Chen, J. H.; Baldi, P. Learning to Predict Chemical Reactions. *J. Chem. Inf. Model.* **2011**, *51*, 2209–2222. (b) Kayala, M. A.; Baldi, P. Reaction Predictor: Prediction of Complex Chemical Reactions at the Mechanistic Level Using Machine Learning. *J. Chem. Inf. Model.* **2012**, *52*, 2526–2540. (c) Fooshee, D.; Mood, A.; Gutman, E.; Tavakoli, M.; Urban, G.; Liu, F.; Huynh, N.; Van Vranken, D.; Baldi, P. Deep Learning for Chemical Reaction Predictions. *Mol. Syst. Des. Eng.* **2018**, *3*, 442–452.
- (5) Tavakoli, M.; Baldi, P. Continuous Representation of Molecules Using Graph Variational Autoencoder. arXiv:2004.08152 (cs).
- (6) Hoffmann, G.; Balcilar, M.; Tognetti, V.; Héroux, B. G.; Adam, S.; Joubert, L. Predicting experimental electrophilicities from quantum and topological descriptors: A machine learning approach. *J. Comput. Chem.* 2020, 41, 2124–2136.
- (7) Chen, J. H.; Baldi, P. No Electron Left-Behind: A Rule-based Expert System to Predict Chemical Reactions and Reaction Mechanisms. *J. Chem. Inf. Model.* **2009**, 49, 2034–2043.
- (8) Phan, T. B.; Breugst, M.; Mayr, H. Towards a general scale of nucleophilicity? *Angew. Chem., Int. Ed.* **2006**, *45*, 3869–3874.
- (9) Mayr, H.; Ofial, A. R. Do general nucleophilicity scales exist? *J. Phys. Org. Chem.* **2008**, *21*, 584–595.
- (10) Ofial, A. R. Mayr's Database Of Reactivity Parameters: Searches, 2015; www.cup.lmu.de/oc/mayr/reaktionsdatenbank2/ (September 29, 2020).
- (11) Wang, C.; Fu, Y.; Guo, Q.-X.; Liu, L. First-Principles Prediction of Nucleophilicity Parameters for pi Nucleophiles: Implications for Mechanistic Origin of Mayr's Equation. *Chem. Eur. J.* **2010**, *16*, 2586–2598.
- (12) Brønsted, J. N.; Pederson, K. Die katalytische Zersetzung des Nitramids und ihre physikalisch-chemische Bedeutung. *Z. Phys. Chem.* **1924**, *108U*, 185–253.
- (13) Edwards, J. O. Correlation of Relative Rates and Equilibria with a Double Basicity Scale. *J. Am. Chem. Soc.* **1954**, *76*, 1540–1547.
- (14) Edwards, J. O. Polarizability, Basicity and Nucleophilic Character. J. Am. Chem. Soc. 1956, 78, 1819–1820.
- (15) Brotzel, F.; Chu, Y. C.; Mayr, H. Nucleophilicities of Primary and Secondary Amines in Water. J. Org. Chem. 2007, 72, 3679–3688.
- (16) Bunting, J. W.; Mason, J. M.; Heo, C. K. M. Nucleophilicity towards a saturated carbon atom: rate constants for aminolysis of methyl 4-nitrobenzenesulfonate in aqueous solution: A comparison of the n and N+ parameters for amine nucleophilicity. *J. Chem. Soc., Perkin Trans.* 2 **1994**, 2291–2300.
- (17) Heo, C. K. M.; Bunting, J. W. Nucleophilicity Towards a Vinylic Carbon Atom: Rate Constants for the Additions of Amines to the 1-Methyl-4-Vinylpyridinium Cation in Aqueous Solution. *J. Chem. Soc., Perkin Trans.* 2 **1994**, 2279–2290.
- (18) Hall, H. K., Jr.; Bates, R. B. Correlation of Alkylamine Nucleophilicities With Their Basicities. *Tetrahedron Lett.* **2012**, *53*, 1830–1832.
- (19) $\log k$ for nucleophilic addition was determined using the Mayr equation for a diverse set of nucleophiles. See the Supporting Information.
- (20) An, F.; Maji, B.; Min, E.; Ofial, A. R.; Mayr, H. Basicities and Nucleophilicities of Pyrrolidines and Imidazolidinones Used as Organocatalysts. *J. Am. Chem. Soc.* **2020**, *142*, 1526–1547.
- (21) Bug, T.; Mayr, H. Nucleophilic Reactivities of Carbanions in Water: The Unique Behavior of the Malodinitrile Anion. *J. Am. Chem. Soc.* **2003**, *125*, 12980–12896.
- (22) Kütt, A.; Selberg, S.; Kaljurand, I.; Tshepelevitsh, S.; Heering, A.; Darnell, A.; Kaupmees, K.; Piirsalu, M.; Leito, I. pK_a values in organic chemistry Making maximum use of the available data. *Tetrahedron Lett.* **2018**, *59*, 3738–3748.
- (23) Bordwell, F. G. Equilibrium Acidities in Dimethyl Sulfoxide Solution. *Acc. Chem. Res.* **1988**, 21, 456–463.
- (24) Klamt, A.; Eckerty, F.; Diedenhofen, M. First Principles Calculations of Aqueous pK_a Values for Organic and Inorganic Acids Using COSMO–RS Reveal an Inconsistency in the Slope of the pK_a Scale. *J. Phys. Chem. A* **2003**, *107*, 9380–9386.

- (25) Ding, F.; Smith, J. M.; Wang, H. First-Principles Calculation of pK_a Values for Organic Acids in Nonaqueous Solution. *J. Org. Chem.* **2009**, 74, 2679–2691.
- (26) Almerindo, G. I.; Tondo, D. W.; Pilego, J. R. Ionization of Organic Acids in Dimethyl Sulfoxide Solution: A Theoretical *Ab Initio* Calculation of the pK_a Using a New Parametrization of the Polarizable Continuum Model. *J. Phys. Chem. A* **2004**, *108*, 166–171.
- (27) Trummal, A.; Rummel, A.; Lippmaa, E.; Koppel, I.; Koppel, I. A. Calculations of pK_a of Superacids in 1,2-Dichloroethane. *J. Phys. Chem. A* **2011**, *115*, 6641–6645.
- (28) Campodónico, P. R.; Aizman, A.; Contreras, R. Electrophilicity of quinones and its relationship with hydride affinity. *Chem. Phys. Lett.* **2009**, 471, 168–173.
- (29) Mood, A.; Tavakoli, M.; Gutman, E.; Kadish, D.; Baldi, P.; Van Vranken, D. L. Methyl Anion Affinities of the Canonical Organic Functional Groups. *J. Org. Chem.* **2020**, *85*, 4096–4102.
- (30) Hine, J.; Weimar, R. J. Carbon Basicity. J. Am. Chem. Soc. 1965, 87, 3387–3396.
- (31) Deakyne, C. A.; Meot-Ner, M. Methyl Cation Affinities of N, O, and C Lone-Pair Donors. *J. Phys. Chem.* **1990**, *94*, 232–239.
- (32) Wei, Y.; Singer, T.; Mayr, H.; Sastry, G. N.; Zipse, H. Assessment of Theoretical Methods for the Calculation of Methyl Cation Affinities. *J. Comput. Chem.* **2008**, *29*, 291–297.
- (33) Lindner, C.; Maryasin, B.; Richter, F.; Zipse, H. Methyl cation affinity (MCA) values for phosphanes. *J. Phys. Org. Chem.* **2010**, 23, 1036–1042.
- (34) Lindner, C.; Tandon, R.; Maryasin, B.; Larionov, E.; Zipse, H. Cation affinity numbers of Lewis bases. *Beilstein J. Org. Chem.* **2012**, *8*, 1406–1442.
- (35) Follet, E.; Zipse, H.; Lakhdar, S.; Ofial, A. R.; Berionni, G. Nucleophilicities and Lewis Basicities of Sterically Hindered Pyridines. *Synthesis* **2017**, *49*, 3495–3504.
- (36) Pellerite, M. J.; Brauman, J. I. Intrinsic Barriers in Nucleophilic Displacements. A General Model for Intrinsic Nucleophilicity toward Methyl Centers. *J. Am. Chem. Soc.* **1983**, *105*, 2672–2680.
- (37) Mayr, H.; Breugst, M.; Ofial, A. R. Farewell to the HSAB Treatment of Ambident Reactivity. *Angew. Chem., Int. Ed.* **2011**, *50*, 6470–6505.
- (38) Aggarwal, V. K.; Mereu, A. Superior Amine Catalysts for the Baylis-Hillman Reaction: The Use of DBU and its Implications. *Chem. Commun.* **1999**, 2311–2312.
- (39) Wei, Y.; Sastry, G. N.; Zipse, H. Methyl Cation Affinities of Commonly Used Organocatalysts. *J. Am. Chem. Soc.* **2008**, *130*, 3473–3477.
- (40) Maji, B.; Breugst, M.; Mayr, H. N-Heterocyclic Carbenes: Organocatalysts with Moderate Nucleophilicity but Extraordinarily High Lewis Basicity. *Angew. Chem., Int. Ed.* **2011**, *50*, 6915–6919.
- (41) Levens, A.; An, F.; Breugst, M.; Mayr, H.; Lupton, D. W. Influence of the N-Substituents on the Nucleophilicity and Lewis Basicity of N-Heterocyclic Carbenes. *Org. Lett.* **2016**, *18*, 3566–3569.
- (42) Maji, B.; Breugst, M.; Mayr, H. N-Heterocyclic Carbenes: Organocatalysts with Moderate Nucleophilicity but Extraordinarily High Lewis Basicity. *Angew. Chem., Int. Ed.* **2011**, *50*, 6915–6919.
- (43) Mayr, H.; Lakhdar, S.; Maji, B.; Ofial, A. R. A quantitative approach to nucleophilic organocatalysis. *Beilstein J. Org. Chem.* **2012**, *8*, 1458–1478.
- (44) Mayr, H. Reply to T. W. Bentley: Limitations of the s(E + N) and Related Equations. *Angew. Chem., Int. Ed.* **2011**, *50*, 3612–3618.
- (45) Brauman, J. I.; Dodd, J. A.; Han, C.-C. Intrinsic Nucleophilicity. In *Nucleophilicity*; Harris, J. M., McManus, S. P., Eds.; ACS Publications: Washington, DC, 1987; Chapter 2, pp 23–33.
- (46) Baidya, M.; Horn, M.; Zipse, H.; Mayr, H. Organocatalytic Activity of Cinchona Alkaloids: Which Nitrogen Is More Nucleophilic. J. Org. Chem. 2009, 74, 7157–7164.
- (47) Hoz, S.; Basch, H.; Wolk, J. L.; Hoz, T.; Rozenthal, E. Intrinsic Barriers in Identity $S_{\rm N}^2$ Reactions and the Periodic Table. *J. Am. Chem. Soc.* **1999**, *121*, 7724–7725.
- (48) Ammer, J.; Nolte, C.; Mayr, H. Free Energy Relationships for Reactions of Substituted Benzhydrylium Ions: From Enthalpy over

- Entropy to Diffusion Control. *J. Am. Chem. Soc.* **2012**, *134*, 13902–13911.
- (49) Sokolov, A. Y.; Mittal, S.; Simmonett, A. C.; Schaefer, H. F., III Characterization of the *t*-Butyl Radical and Its Elusive Anion. *J. Chem. Theory Comput.* **2012**, *8*, 4323–4329.
- (50) Breslow, R.; Grant, J. L. Electrochemical determination of the basicities of benzyl, allyl, and propargyl anions, and a study of solvent and electrolyte effects. *J. Am. Chem. Soc.* **1977**, *99*, 7745–7746.
- (51) Ali, A.; Sittler, E. C., Jr.; Chornay, D.; Rowe, B. R.; Puzzarini, C. Organic chemistry in Titan's upper atmosphere and its astrobiological consequences: I. Views towards Cassini plasma spectrometer (CAPS) and ion neutral mass spectrometer (INMS) experiments in space. *Planet. Space Sci.* **2015**, *109–110*, 46–63.
- (52) Oliveira, A. M.; Lu, Y.-J.; Lehman, J. H.; Changala, P. B.; Baraban, J. H.; Stanton, J. F.; Lineberger, W. C. Photoelectron Spectroscopy of the Methide Anion: Electron Affinities of ●CH₃ and ●CD₃ and Inversion Splittings of CH₃[−] and CD₃[−]. *J. Am. Chem. Soc.* **2015**, *137*, 12939−12945.
- (53) TURBOMOLE V7.3 2018, a development of University of Karlsruhe and Forschungszentrum Karlsruhe GmbH, 1989–2007, TURBOMOLE GmbH, since 2007; available from http://www.turbomole.com.
- (54) Becke, A. D. Density-functional exchange-energy approximation with correct asymptotic behavior. *Phys. Rev. A: At., Mol., Opt. Phys.* **1988**, 38, 3098–3100.
- (55) (a) Burke, K.; Perdew, J. P.; Ernzerhof, M. Generalized gradient approximation made simple. *Phys. Rev. Lett.* **1996**, 77, 3865–3868. (b) Adamo, C.; Barone, V. C. Toward reliable density functional methods without adjustable parameters: The PBE0 model. *J. Chem. Phys.* **1999**, 110, 6158–6169.
- (56) (a) Grimme, S.; Erhrlich, A. S.; Krieg, H. A consistent and accurate *ab initio* parametrization of density functional dispersion correction (DFT-D) for the 94 elements H-Pu. *J. Chem. Phys.* **2010**, 132, 154104–19. (b) Grimme, S.; Ehrlich, S.; Goerigk, L. Effect of the damping function in dispersion corrected density functional theory. *J. Comput. Chem.* **2011**, 32, 1456–1465.
- (57) Klamt, A. The COSMOS and COSMO-RS. WIREs Comput. Mol. Sci. 2018, 8, e1338.
- (58) Klamt, A.; Jonas, V.; Bürger, T.; Lohrenz, J. C. W. Refinement and parametrization of COSMO-RS. J. Phys. Chem. A 1998, 102, 5074–5085.